

## BL13XU

### X-ray Diffraction and Scattering I

#### 1. Introduction

So far, various X-ray diffraction systems have been developed across several beamlines in SPring-8 because X-ray diffraction is one of the most powerful tools to investigate the crystallographic structure of materials at the atomic scale. Recently, the demand for advanced techniques such as in situ, operando, and automatic measurements by many users in various fields has been increasing. To accommodate these demands, it is necessary to integrate and rearrange the diffraction systems in each beamline. Therefore, the restructuring of the X-ray diffraction beamlines had been planned by a special working group.

In the restructuring plan put forth by the working group, the upgrades in BL13XU were promoted for the beginning of FY2022. The beamline was renamed “X-ray Diffraction and Scattering I”. BL13XU contains a multi-axis diffractometer at Experimental hutch 1, a diffraction measurement multipurpose frame at hutch 2, a high-resolution powder diffractometer at hutch 3, and nanodiffraction system at hutch 4 after the upgrade. The beamline optics were also upgraded for the application of high-energy X-rays. We describe the details of the upgrades below.

#### 2. Upgrades of the beamline optics

Before the upgrades, BL13XU was designed for X-rays from 6 to 50 keV. Recently, X-rays with higher energy have been required by many users because of their advantages such as accessibility to a wide reciprocal space and the possibility of using transmission diffraction geometry. The rapid

improvement of the area detector also accelerates this trend. To achieve the application of higher-energy X-rays, the optical components of the beamline were upgraded for using X-rays up to 72 keV.

In the upgrade, modification of the monochromator was applied. Si(111) and Si(311) crystals were installed as monochromator crystals; these can be exchanged in accordance with the X-ray energy. Si(311) is used for X-rays of over 37 keV, whereas Si(111) is used for X-rays of lower energy. The mirrors, which focus X-rays to the sample position and eliminate higher-order harmonics, were also renewed. The mirrors are made of silicon crystals, the upper half of which is coated with Pt for high-energy X-rays of over 17 keV. As the control system of the optics, BL-774, a new beamline control platform, was installed for future application to remote experiments.

Figure 1 shows the photon flux at BL13XU. It is clear that high flux is obtained over 40 keV. For example, the flux exceeding  $10^{10}$  photon/s is obtained at 72 keV.

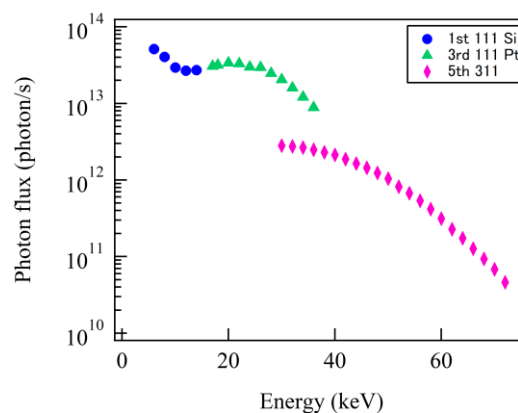


Fig. 1. Photon flux under the typical condition in BL13XU.

### 3. Multi-axis diffractometer

The versatile six-axis diffractometer, also known as the Huber multi-axis diffractometer, along with its peripheral instruments, which had previously been installed and operated in EH1 at BL46XU, were relocated to EH1 at BL13XU in March 2022. User beamtime was resumed in June 2022 after completing the offline startup of the diffractometer and peripherals, conducting on-beam adjustments to the optics, and performing test measurements with standard experimental setups. The first 11 experimental proposals were implemented during

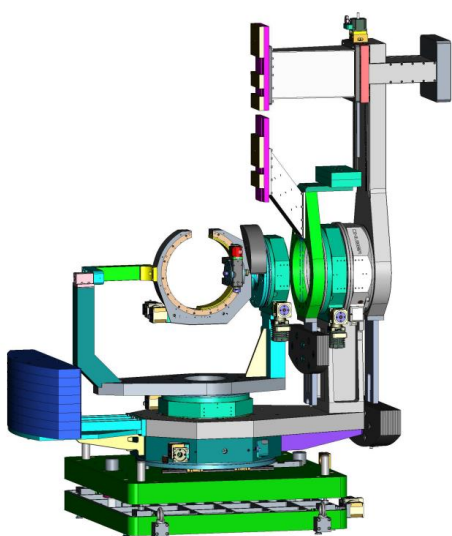


Fig. 2. (top) Versatile multi-axis diffractometer installed in EH1. (bottom) CAD drawing of the diffractometer.

the 2022A term. Until the 2021B term, the device had been accessible exclusively for proposals within the industrial and industry–academia collaboration application field. However, starting from the 2022A term, it has been open to proposals spanning academic and other applications in diverse scientific fields.

As illustrated in Fig. 2, the diffractometer is composed of eight primary axes (four basic  $\chi$ ,  $\phi$ ,  $\omega$ , and  $2\theta$  axes and four additional  $2\theta_z$ ,  $\theta_z$ ,  $\omega_a$ , and  $2\theta_a$  axes), along with a secondary detector arm featuring two axes ( $2\theta_2$  and  $2\theta_{z2}$ ). An analyzer stage is installed on the detector arm with the  $\omega_a$  and  $2\theta_a$  axes. The available analyzer crystals are Si (111), Ge (111), and LiF (002) [1]. An open  $\chi$  cradle is utilized to achieve a broad scattering angular range ( $-20^\circ$  to  $160^\circ$ ) while avoiding dead angles. Samples can be placed on a motorized XYZ and/or swivel stage, enabling precise sample positioning adjustments as well as mapping measurements of irradiated positions. In the optical setup, there are a total of three motorized four-quadrant slits: one is positioned on the upstream side of the diffractometer for beam size adjustment, and the other two are located on the detector arm to control the collimation of the detected signal. The height and width of the incident beam can be adjusted in accordance with the experiment's objectives. The smallest and largest beam sizes achievable using the slit are approximately  $30\ \mu\text{m} \times 30\ \mu\text{m}$  and  $0.7\ \text{mm} \times 1.0\ \text{mm}$ , respectively. A microbeam approximately  $3\ \mu\text{m} \times 10\ \mu\text{m}$  in size can be made using X-ray focusing elements such as a zone plate or refractive lens.

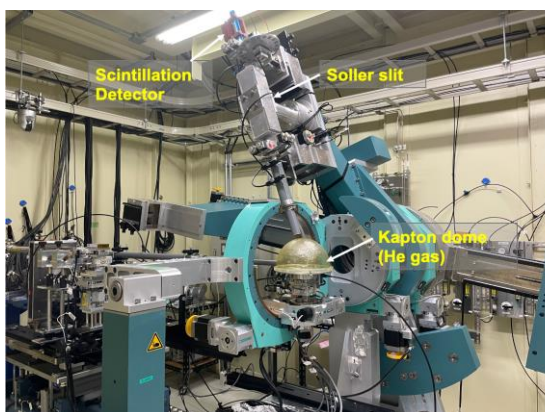


Fig. 3. Grazing-incidence X-ray scattering setup at the beamline BL13XU.

As shown in Fig. 3, a solar slit can be inserted on the analyzer stage to enhance the detection efficiency of scattering signals from a broader irradiation area on the thin-film sample surface during grazing-incident X-ray scattering measurements. Two attenuator autochangers have been installed, with one located on the upstream side and the other on the detector arm just before the detector. The detector can be chosen from 0-dimensional (LaBr<sub>3</sub> scintillation and NaI scintillation) [2], 1-dimensional (6 modules of MYTEHN), and 2-dimensional (PILATUS 100K, 300K, and 2M) detectors. This provides the capability for conducting versatile X-ray diffraction experiments. As depicted in Fig. 3, the sample can be mounted on a stage within a Kapton dome chamber filled with helium gas to effectively minimize background noise caused by air scattering around the sample. X-ray diffraction measurements can be conducted under various nonambient conditions by adjusting the sample environmental parameters, including temperature using the Anton Paar DHS1100 (room temperature to 1100 °C) and Anton Paar DCS500 (−180 to 500 °C), as well as

mechanical loading using a tensile tester with 2 kN and 200 N load cells. SPEC (Certified Scientific Software) is utilized for controlling the beamline and the diffractometer.

#### 4. Diffraction measurement multi-purpose frame

In recent applications of X-ray diffraction, demands for the control of the sample environment have been increasing, such as heating, cooling, and impression of voltage. In addition, in situ and operando measurements during the sample processing or device operation are desired. These sophistications make sample environment devices large and heavy. In the traditional diffractometer, however, it is difficult to mount large sample devices because the space around the sample is limited by the rotational stages such as the  $\chi$ -circle and two-theta arm. For this reason, we designed a new type of diffraction system named “diffraction measurement multipurpose frame” to secure sufficient space around the sample.

The multipurpose frame is mainly composed of the sample stage and a robot arm (Fig. 4). The sample stage is a combination of XZ stages,

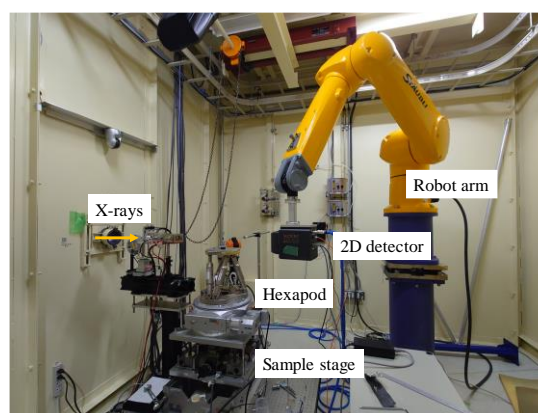


Fig. 4. Photograph of the diffraction measurement multipurpose frame.

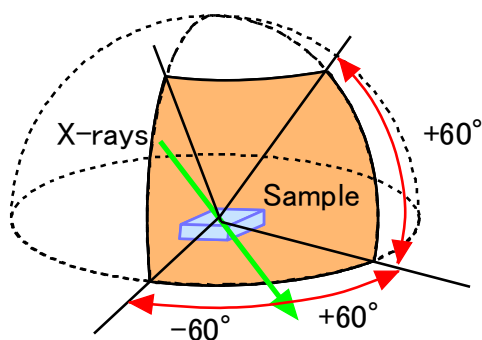


Fig. 5. Accessible angle of the detector via the robot arm at a camera distance of 1 m.

rotational stage, and hexapod. The hexapod is loaded on the stages for translation along X, Y, and Z axes and rotation around Rx, Ry, and Rz axes independently. The maximum load of the sample stage is 250 kg.

The robot arm for the area detector is combined with the sample stage. The robot arm has a maximum load of 25 kg and a reach of 2 m. The camera distance from the sample to the detector can be controlled from 150 to 1000 mm. When the camera distance is aligned at 1000 mm, the robot arm can cover the scattering angle of  $\pm 60^\circ$  in the horizontal direction and  $60^\circ$  in the vertical direction (Fig. 5). PILATUS X 300k is mounted at the tip of the robot arm.

This apparatus is designed for users who carry in their own sample environment devices to the beamline. Because of the wide space around the sample position, not only they can bring in the device they usually use in their laboratory, but they can also freely design devices for in situ/operando measurements without a space limitation.

### 5. High-resolution powder diffractometer

The high-resolution powder diffractometer newly

installed in the third hutch is designed to meet the diverse needs of academic and industrial users for X-ray diffraction and scattering analyses under various sample conditions using X-ray energy from 16 to 72 keV. Previously, a high-throughput powder diffractometer with diverse automated techniques was developed at the bending magnet beamline BL02B2, SPring-8. This development has enabled users to consistently obtain high-quality outcomes. Enhancement targets include i) reducing the measurement time to under one second, ii) investigating partly disordered materials, iii) extending the  $Q$ -range beyond  $20 \text{ \AA}^{-1}$ , and iv) accommodating a sample environment greater than 100 mm. To address these issues, we have introduced a new powder diffractometer at ID beamline BL13XU, designed for higher throughput measurements, in situ and operando experiments, and data acquisition for pair distribution function (PDF) analysis. In addition to automatic powder diffraction measurements, the system is coordinated with an automatic powder filling system for capillary sample preparation, ensuring that a series of tasks and measurements in powder diffraction are fully automated. The system also features an automatic equipment switching mechanism. It can accommodate equipment with sides up to approximately 600 mm and a weight capacity of about 300 kg on its large sample stage ( $\theta$ , XYZ-axes). The apparatus/system has a mechanism to automatically insert this stage towards the diffractometer side. This mechanism enables various in situ/operando X-ray diffraction experiments using a large sample space.

Figure 6 presents a photograph of the developed powder diffractometer system. The diffractometer operates on a  $\theta/2\theta$ -axis and is



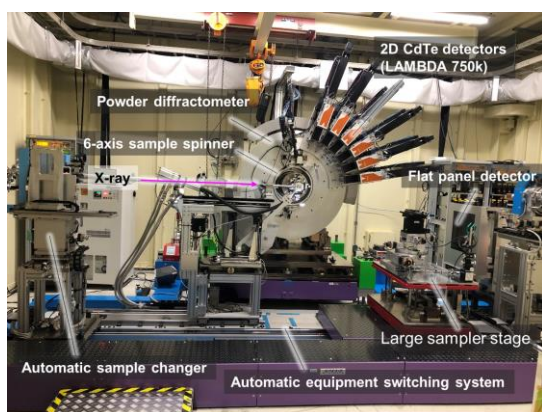


Fig. 6. Picture of new high-resolution powder diffractometer at EH3.

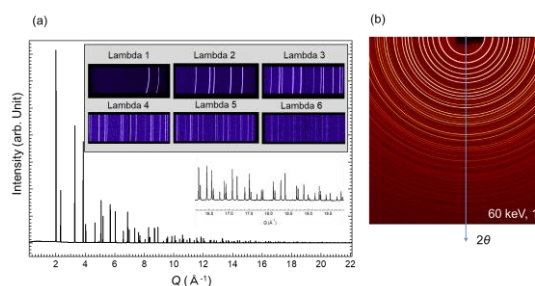


Fig. 7. (a) Powder diffraction data of  $\text{CeO}_2$  measured with six sets of LAMBDA 750k detectors. The inset shows a portion of the 2D diffraction image. (b) 2D powder diffraction data of  $\text{LaB}_6$  measured with a large-area flat-panel detector.

equipped with a motorized 6-axis high-speed spinner (200 rpm) sample stage. It is feasible to mount a compact sample cell on the spinner sample stage, and in terms of many types of equipment, such as sample holders, it possesses compatibility with the powder diffractometer at BL02B2. On the  $2\theta$ -axis, six sets of two-dimensional CdTe (LAMBDA 750k) detectors with high efficiency for high-energy X-rays are mounted with adjustability

ranging from 500 to 1100 mm. The typical distances between the sample and the detector are 630 mm and 1050 mm, with angular resolutions  $\Delta 2\theta$  of  $0.005^\circ$  and  $0.003^\circ$ , respectively. The detectable  $2\theta$  range is from  $1^\circ$  to  $80^\circ$ , and for in situ/operando measurements in the single-shot mode, a range from  $1^\circ$  to  $40^\circ$  can be utilized. Furthermore, powder diffraction experiments in which the temperature control unit and the large-area detector unit are combined are available. The flat-panel detector is mounted on the XYZ stage on the large-area detector unit, and the distance between the sample and the detector can be adjusted from 400 to 1800 mm. Figure 7(a) shows the powder diffraction data of a  $\text{CeO}_2$  sample measured at 35 keV using the LAMBDA 750k detector, whereas Fig. 7(b) displays the powder diffraction data of a  $\text{LaB}_6$  sample measured at 60 keV using the large-area flat-panel detector. These data were obtained with exposure times of 1 and 10 s, respectively, and are sufficient for crystal structure analysis even with a short exposure time of 1 s. Regarding the sample environment, nitrogen-gas low-temperature/high-temperature blower devices are usually installed. This allows for temperatures ranging from 90 to 1100 K. In combination with an automatic sample exchanger, automatic measurements of up to 100 samples, including samples at various temperature, are possible. In addition, a remote gas handling system, which can control the various sample gas environments, synchronized with measurements, has been introduced.

## 6. Nanodiffraction system (Experimental hutch 4)

In the upgrade, the nanodiffraction system is not modified<sup>[3]</sup>. The schematic is shown in Fig. 8. A

Fresnel zone plate (FZP) and compound refractive lenses (CRLs) are installed on the system as

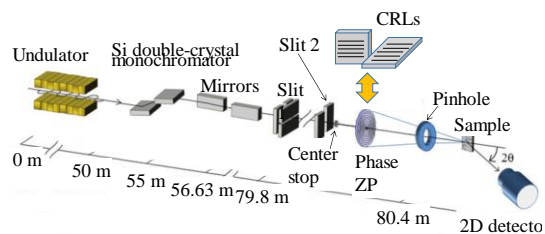


Fig. 8. Schematic of the nanodiffraction system.

focusing devices.

The renewal of the mirrors made the incident X-rays uniform and improved the flux and stability of the focused beam. In the case of 8 keV, the flux of the X-rays focused by the FZP is several times higher than before the upgrade.

#### Authors

Sumitani Kazushi<sup>1</sup>, Koganezawa Tomoyuki<sup>1,2</sup>, & Kawaguchi Shogo<sup>1</sup>

<sup>1</sup>Diffraction and Scattering Division, JASRI

<sup>2</sup>Industrial Application and Partnership Division, JASRI

#### References:

- [1] Nakayama, Y. Nakanishi, Y. Kumara, R. & Koganezawa, T. (2023). *J. Cryst. Growth* **621**, 127365.
- [2] Toyama, R. et al. (2023). *Phys. Rev. Mater.* **7**, 084401.
- [3] Imai, Y. Sumitani, K. & Kimura, S. (2019). *AIP Conf. Proc.* **2054**, 050004